

## Evaluation of Acoustic Properties of Amorphous Ta<sub>2</sub>O<sub>5</sub> Thin Film Prepared by RF Sputtering

高周波スパッタリング法により作製されたアモルファス Ta<sub>2</sub>O<sub>5</sub> 薄膜の音響特性評価

Shoji Kakio<sup>1†</sup>, Keiko Hosaka<sup>1</sup>, Mototaka Arakawa<sup>2</sup>, Yuji Ohashi<sup>2</sup>, and Jun-ichi Kushibiki<sup>2</sup>  
(<sup>1</sup>Univ. of Yamanashi; <sup>2</sup>Tohoku Univ.)

垣尾 省司<sup>1†</sup>, 保坂 桂子<sup>1</sup>, 荒川 元孝<sup>2</sup>, 大橋 雄二<sup>2</sup>, 櫛引 淳一<sup>2</sup> (山梨大院・医工, <sup>2</sup>東北大院・工)

### 1. Introduction

An amorphous Ta<sub>2</sub>O<sub>5</sub> thin film has a high refractive index and a high density compared with other dielectric thin-film materials. A Ta<sub>2</sub>O<sub>5</sub>/SiO<sub>2</sub> multilayer structure has been widely used in the field of optical devices. Kushibiki *et al.* are developing an optical cavity using a Ta<sub>2</sub>O<sub>5</sub>/SiO<sub>2</sub> multilayer mirror with low loss and high reflectivity to realize next-generation optical frequency standards. To improve the quality of optical cavities, it is necessary to clarify the correlation among the extinction coefficient of the materials in the multilayer, the absorption and scattering losses of the multilayer, and the fabrication process.<sup>1</sup>

On the other hand, in the field of surface acoustic wave (SAW) devices, it has been reported that trapping effects, such as a transformation to a Love-type SAW and an increase in the coupling factor, can be achieved by loading a LiNbO<sub>3</sub> (LN) or quartz substrate with an amorphous Ta<sub>2</sub>O<sub>5</sub> thin film with a thickness of a few percent of the wavelength.<sup>2-5</sup> However, optimization of the deposition conditions to improve the propagation loss and temperature coefficient is required.

In this paper, the fundamental acoustic properties of amorphous Ta<sub>2</sub>O<sub>5</sub> thin film prepared by RF sputtering were evaluated from the propagation properties of SAWs excited by interdigital transducers (IDTs) and from those of a leaky SAW (LSAW) analyzed by a line-focus beam ultrasonic material characterization (LFB-UMC) system.<sup>6</sup>

kakio@yamanashi.ac.jp

### 2. Sample Fabrication

An amorphous Ta<sub>2</sub>O<sub>5</sub> thin film was deposited on a 128° YX-LN, 36° YX-LiTaO<sub>3</sub> (LT), or SiO<sub>2</sub> glass substrate using an ANELVA SPF-210A or SPF-201H RF magnetron sputtering system (equipment A or B, respectively) without substrate heating under the sputtering conditions shown in **Table I**.

For conditions A1-A3 and B1-B3, samples with film thicknesses  $H$  of approximately 2.5 and 5.0  $\mu\text{m}$  were fabricated on both LN and LT substrates. For the A0 condition, samples with several film thicknesses ranging from 0.96 to 5.44  $\mu\text{m}$  were fabricated on an LN substrate. IDTs with a period  $\lambda$  of 20  $\mu\text{m}$  and 8 split-finger pairs were fabricated on the samples using a 0.01 $\lambda$ -thick Al film. Moreover, samples with several film thicknesses ranging from 1.0 to 9.7  $\mu\text{m}$  and a sample with a film thickness of 5.0  $\mu\text{m}$  were also fabricated under the A0 and B0 conditions, respectively, on SiO<sub>2</sub> glass substrates.

### 3. Evaluation of Acoustical Physical Constants

The phase velocity was determined by multiplying  $\lambda$  by the center frequency of the measured frequency response between the IDTs. **Figures 1(a) and 1(b)** show the measured phase velocities of the Rayleigh wave on the 128° YX-LN ( $V_{\text{Rayleigh}}$ ) and the shear horizontal (SH)-type SAW on 36° YX-LT ( $V_{\text{SH-SAW}}$ ), respectively, as functions of the normalized film thickness  $H/\lambda$ . A marked difference was observed between the dispersion curves of the SAWs obtained using equipment A and B.

Table I. Deposition conditions and evaluated acoustical physical constants.

Condition	Target	RF Power [W]	Ar:O <sub>2</sub> [ccm]	Pressure [Pa]	Depo. Rate [ $\mu\text{m}/\text{h}$ ]	$\rho \times 10^3$ [ $\text{kg}/\text{m}^3$ ]	$c_{11} \times 10^{11}$ [ $\text{N}/\text{m}^2$ ]	$c_{44} \times 10^{11}$ [ $\text{N}/\text{m}^2$ ]
A0	Ta 3 inch $\phi$	200	4:1	1.3	0.41	5.0	-	-
A1		300	4:1	1.3	0.58	5.0	1.31	0.39
A2			5:1	1.3	0.62	5.0	1.30	0.40
A3			5:1	3.0	0.70	5.1	1.40	0.41
B0	Ta 4 inch $\phi$	200	5:1	2.0	0.63	-	-	-
B1			4:1	2.0	0.66	7.3	1.60	0.44
B2			4:2	2.0	0.62	7.3	1.53	0.44
B3			4:2	3.0	0.57	7.2	1.53	0.43

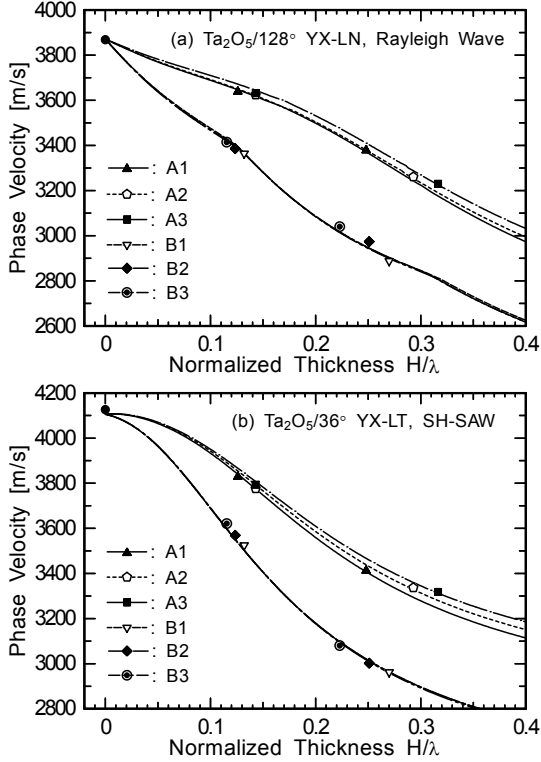


Fig. 1 Phase velocity vs  $H/\lambda$  for (a) Rayleigh wave on  $128^\circ$  YX-LN and (b) SH-SAW on  $36^\circ$  YX-LT.

Then, the elastic constants of the  $\text{Ta}_2\text{O}_5$  thin film were determined by the following procedure. First, the relative dielectric constant  $\epsilon/\epsilon_0=19.5$  was adopted because it is the closer value to the reported value<sup>7</sup> for an insulator film ( $\epsilon/\epsilon_0=18-24$ ) among the reported values<sup>8</sup> for an X-axis oriented  $\text{Ta}_2\text{O}_5$  thin film. Next, the density  $\rho$  was determined by measuring the increase in mass after deposition. Then,  $c_{11}$  and  $c_{44}$  were determined simultaneously so that the difference in the square of the errors between the calculated and measured phase velocities for the Rayleigh wave on the  $128^\circ$  YX-LN and the SH-SAW on  $36^\circ$  YX-LT was minimized. The elastic constants and density of the samples are shown in Table I. The phase velocities calculated using the obtained constants are also shown in Figs. 1(a) and 2(a). The  $\text{Ta}_2\text{O}_5$  thin film deposited using equipment B has a higher density and larger elastic constants than that deposited by equipment A. When sputtering parameters such as the gas pressure and  $\text{O}_2$  gas ratio were varied while using the same equipment, no major change in the acoustical physical constants was observed.

#### 4. Evaluation by LFB-UMC System

The phase velocity  $V_{\text{LSAW}}$  and normalized attenuation factor  $\alpha_{\text{LSAW}}$  of the LSAWs on the LN sample obtained under the A0 condition after removing the IDTs and those for the  $\text{SiO}_2$  sample were determined from  $V(z)$  curves, which were measured by the LFB-UMC system at an ultrasonic frequency  $f$  of 100-300 MHz.

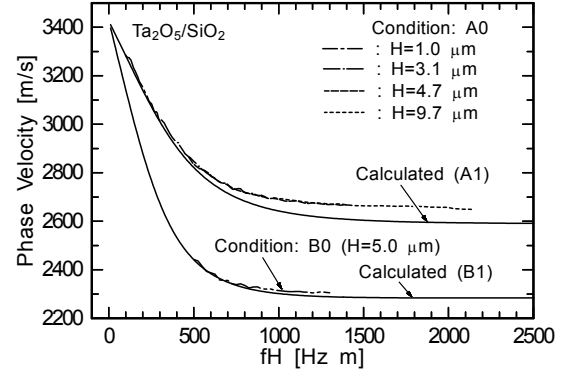


Fig. 2 Phase velocity vs  $fH$  for LSAW on  $\text{SiO}_2$ .

For the LN sample, the  $fH$  dependence, that is, the dispersion curve of  $V_{\text{LSAW}}$ , agreed with that of  $V_{\text{Rayleigh}}$ . Figure 2 shows the dispersion curve of  $V_{\text{LSAW}}$  on the  $\text{SiO}_2$  sample. The convergent value of  $V_{\text{LSAW}}$  for the B0 condition is approximately 380 m/s less than that for the A0 condition. Thus, a difference between the acoustic properties obtained using equipment A and B was clearly detected.

The dispersion curves calculated using the evaluated acoustical physical constants for the A1 and B1 conditions are also shown in Fig. 2. The convergent value of the calculated  $V_{\text{LSAW}}$  for the A1 condition is approximately 60 m/s less than the measured value for the A0 condition. This difference is considered to be caused by the difference in the deposition conditions (RF power: 200 or 300 W). On the other hand, the calculated dispersion curve for the A1 condition agreed with the measured curve because there are no major changes in the acoustical physical constants when the  $\text{O}_2$  gas ratio is varied. Furthermore, for both equipment A and B, the calculated  $fH$  dependences of  $\alpha_{\text{LSAW}}$  also agreed well with the measured values.

#### 5. Conclusions

The fundamental acoustic properties of an amorphous  $\text{Ta}_2\text{O}_5$  thin film prepared by RF sputtering were evaluated. It was found that a  $\text{Ta}_2\text{O}_5$  thin film with a higher density and larger elastic constants can be deposited by equipment with a larger Ta target size. The difference between the acoustic properties of the  $\text{Ta}_2\text{O}_5$  thin film obtained using two sets of equipment was clearly detected by an LFB-UMC system.

#### References

1. M. Arakawa *et al.*: Proc. Piezoelectric Materials and Devices Symp. (2011) 27 [in Japanese].
2. S. Kakio *et al.*: J. Appl. Phys. **87** (2000) 1440.
3. S. Kakio *et al.*: Jpn. J. Appl. Phys. **42** (2003) 3161.
4. S. Kakio *et al.*: Jpn. J. Appl. Phys. **44** (2005) 4544.
5. H. Nakanishi *et al.*: Jpn. J. Appl. Phys. **49** (2010) 07HD21.
6. J. Kushibiki *et al.*: IEEE Trans. UFFC **49** (2002) 99.
7. H. Fujikawa *et al.*: R&D Review of Toyota CRDL **30** (1995) 13 [in Japanese].
8. Y. Nakagawa and T. Okada: J. Appl. Phys. **68** (1990) 556.